



The conditions of the formation and existence of “Blue Ice Areas” in the ice flow transition region from the Antarctic ice sheet to the Amery Ice Shelf in the Larsemann Hills area

Aleksey Markov^{a,*}, Sergey Polyakov^b, Bo Sun^c, Valeriy Lukin^b, Sergey Popov^{d,e}, Huigen Yang^c, Tijun Zhang^c, Xiangbin Cui^c, Jingxue Guo^c, Penghui Cui^c, Li'an Zhang^f, Jamin Greenbaum^g, Andrey Mirakin^b, Andrey Voyevodin^b, Alina Boronina^e, Anastasiya Sukhanova^e, Gennadiy Deshovykh^b, Aleksey Krekhov^e, Sergey Zarin^b, Aleksey Semyonov^b, Vladimir Soshchenko^b, Aleksey Mel'nik^b

^a Polar Research Center, Jilin University, 938 Ximinzhu Str., Changchun, 130021, People's Republic of China

^b Russian Antarctic Expedition, Arctic and Antarctic Research Institute, 38 Bering Str., St. Petersburg, 119397, Russia

^c Polar Research Institute of China, 451 Jinqiao Rd., Shanghai, 200136, People's Republic of China

^d Polar Marine Geosurvey Expedition (PMGE), 24 Pobeda Str., Lomonosov, St. Petersburg, 198412, Russia

^e St Petersburg University, 7–9 Universitetskaya Emb., St Petersburg, 199034, Russia

^f China Airport Construction Group Corporation, 111 Beisihuan East Str., Chaoyang District, Beijing, 100101, People's Republic of China

^g University of Texas at Austin, Institute for Geophysics, 1 University Station, 78712, Austin, TX, USA

ARTICLE INFO

Keywords:

Antarctica
Blue Ice Areas
Ice sheet dynamics
Runway in Antarctica

ABSTRACT

Understanding the trend and main causes of the formation and distribution of Blue ice areas (BIAs) in Antarctica may help the search for areas (BIAs) suitable for ice runways for heavy aircraft. Two districts were explored on the glacier within a 50 km radius around the Larsemann Hills. They were isolated as blue ice areas based on the analysis of satellite images. According to the results of surface studies, one of the areas (about 500x5,000 m in size), though initially identified as a BIA based on the analysis of satellite images, has a high density firn covered with sun crust. The second area is indeed a blue ice area of significant size (about 5,000x5,000 m). Similarities and differences have been determined in the formation conditions of the glacier surface in the two areas of assumed BIAs, and an analysis was carried out to identify dominant, necessary and “sufficient” reasons for the sustained existence of BIAs. An obvious link has been found between the distribution of BIAs and the morphology of the subglacial mountain relief and the ice dynamics.

1. Introduction

The primary research objective was to find BIAs at a distance of no more than 50 km from Progress (Russia) and Zhongshan (China) Stations (Fig. 2.2) that would be suitable for the construction of an ice runway for heavy aircraft and to investigate the parameters of the state and condition of detected BIAs.

The surface of the ice sheet of Antarctica is 99% covered with snow, and only 1% is “open” ice (Bintanja and Reijmer, 2001), which is called “blue ice” due to the characteristic reflected colour of sun rays, and is “scattered” in local areas (Blue Ice Areas - BIAs) across the Antarctic continent (Hui et al., 2014; Winther et al., 2001) (Fig. 1).

BIAs are located mainly near rock exposures (Bintanja, 1999),

which is largely due to the meteorological and morphological conditions of their formation and sustainable existence. BIAs are most widespread, for example, in the large mountain group regions of Antarctica, such as: Transantarctic Mountains, Queen Maud Land, Victoria Land, or in small local mountain group areas, such as: the Vinson Massif and the Grove Mountains (Fig. 1).

At the same time, BIAs are also observed in the marginal coastal zone (Hui et al., 2014), in the “ablation” areas of the ice sheet, or its transition to ice shelves, for example, in such regions as: the Lambert Glacier Basin; the vicinity of Australian Antarctic Stations Casey and Davis (Fig. 1).

In East Antarctica, BIAs also have a multiple distribution in the coastal zone in the form of local small areas, one of which is located in

* Corresponding author. Tel: + 86 431 88502791.

E-mail address: am100@inbox.ru (A. Markov).

<https://doi.org/10.1016/j.polar.2019.08.004>

Received 3 December 2018; Received in revised form 8 August 2019; Accepted 14 August 2019

Available online 26 August 2019

1873-9652/ © 2019 Published by Elsevier B.V.

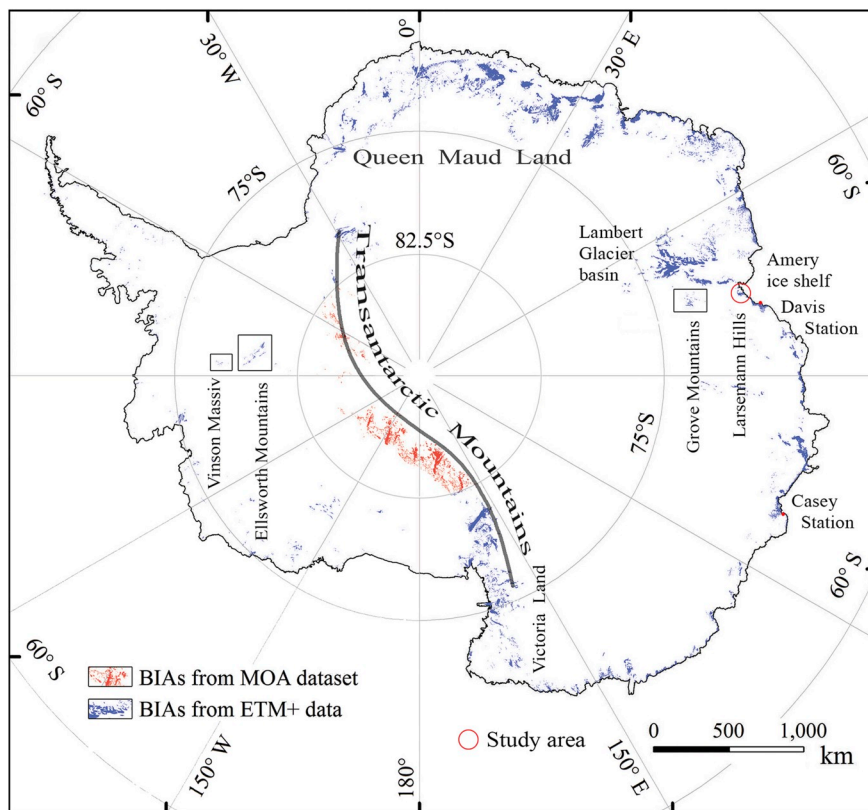


Fig. 1. The distribution of BIAs in Antarctica. The latitude of the circle is 82.5°S, and within the circle (area south of 82.5°S) Landsat has no coverage because of its near-polar orbit. BIAs over the area south of 82.5°S were obtained from the SGS (Snow Grain-Size) image of the MOA (Mosaic of Antarctica), and the others were obtained from Landsat Enhanced TM Plus (ETM+) data (Hui et al., 2014).

the area of our research - in the Larsemann Hills area (Fig. 1). BIAs have a number of unique features that are distinguished from other surfaces of the Antarctic ice sheet (Bintanja, 1999; Bintanja and Reijmer, 2001; Hui et al., 2014; Sinisalo and Moore, 2010; Takahashi et al., 1988; Winther et al., 2001; Winter et al., 2016; Zwinger et al., 2014). BIAs have negative or zero mass balance. They are subject to intensive ablation, most of all due to sublimation. In consequence of this on the surface of the ice sheet the upper "young" layers of ice are destroyed and deeper and "older" layers of ice are observed to the surface. They have higher surface density and hardness. There is less aerodynamic surface texture.

BIAs are of interest for addressing various scientific and engineering challenges. BIAs are useful in paleoclimatic reconstruction (Fireman, 1989; Moore et al., 2006; Nishiizumi et al., 1989; Sinisalo and Moore, 2010; Van Roijen et al., 1995; Whillans and Cassidy, 1983; Zwinger et al., 2014). They provide information in searching for ancient ice (Whillans and Cassidy, 1983). They may be used for airfield construction (Mellor and Swithinbank, 1989). They are good areas for searching for meteorites (Cassidy et al., 1992).

The reasons and conditions for the formation and sustainable existence of BIAs can be divided into the following key categories (Bintanja, 1999; Bintanja and Reijmer, 2001; Hui et al., 2014; Sinisalo and Moore, 2010; Takahashi et al., 1988; Winther et al., 2001; Winter et al., 2016; Zwinger et al., 2014). There is a climatic factor (melting of ice sheet). There are meteorological factors (temperature; wind velocity and turbulence; insolation). There are glaciological factors (snow accumulation balance; the intensity of ablation; aerodynamic surface texture; ice layer structure). Finally, there are orographic factors (the topographic relief of the hills, the bedrock, and the surface of the ice sheet).

All of these factors take part in the formation of BIAs, but the degree of their influence may be different.

The expressed location of BIAs along the periphery of the Antarctic ice sheet is directly connected with the characteristic features of the marginal (transitional) zone of the ice sheet. In this transitional

peripheral zone, there are significant changes in the external conditions compared with the conditions in the central regions of the ice sheet, causing its "dissipation," which can be associated with both the melting and sublimation of the ice and its mechanical destruction. These changes in the conditions and causes of "dissipation" have both a climatic (meteorological) aspect (in particular, higher surface temperature and wind velocity in the periphery of the ice sheet compared with the central regions), and a morphological (topographical) aspect (complex relief of bed rocks), as well as glaciological aspects (structural changes in the occurrence of ice layers and a significant decrease in the total thickness of the ice sheet).

Studying the degree of influence of various causes, conditions and factors of occurrence and the degree of stability of the existence of BIAs allows us to classify and regionalize BIAs. Objective understanding of genesis BIAs, their current status and forecasting future development are important for determining the relationship of the changes BIAs with the variations of climatic conditions and/or with the dynamics of the Antarctic ice sheet.

This work discusses the currently observed conditions for the existence of BIAs in the coastal transition region of ice flow from the Antarctic ice sheet into the Amery Ice Shelf in the Larsemann Hills area.

2. Study area and research data

2.1. Study area

The activities were carried out jointly by Russian and Chinese experts in the season of December 2017–January 2018.

The primary analysis of the probable location of BIAs was made according to a satellite image of 1:200,000 scale detailing about 15 m per pixel (courtesy of V.D. Klokov from the archive of the Arctic and Antarctic Research Institute, Russia) (Fig. 2.2).

At the stage of preliminary analysis according to the logistic task we were interested in areas at a distance of about 40 km from stations that had an intense blue color and a length of about 3 km. Relevant areas

were identified in Regions A and B (red lines in Fig. 2.2).

Region A was conventionally called the Blue Firn Area, and Region B - the Blue Ice Area.

For a more detailed preliminary study of the selected areas, an analysis of higher resolution satellite images was carried out with detailing about 0.5 m per pixel (Fig. 2.3).

The entire region of the general location of both the Blue Firn Area and the Blue Ice Area is characterized by the following features. The region is located on the slope of the coastal “dissipation” of the ice sheet (the thickness of the sheet decreases from 600 m to 300 m). The ice sheet (about 600 m in thickness) is transformed into an ice shelf (about 250–300 m in thickness). The surface height decreases from 900 m to 150 m. The bedrock has mountain relief. Exposures (outcrops) of rocks are not observed.

The Mountain ranges of the bedrock and hills of the ice sheet surface are perpendicular to the ice sheet flow direction (according to results of our airborne radio-echo sounding and satellite observations (Rignot et al., 2011, 2017)). The thickness of the ice sheet in the direction of the ice flow before and above the subglacial mountain range decreases (maximally) from 900 m to 400 m. Elevation difference of the subglacial mountain relief is up to 500 m. The slope of the surface of the subglacial mountain relief is up to 20°. The slope of the upper surface of the ice sheet (total) is up to 3°. Cracks (up to 1,000 m long and up to 50 m wide) are present in the ice sheet (in some places up to 25% of the surface area for an arbitrarily selected square measuring 3 × 3 km). The greatest intensity of cracks in the ice sheet is observed behind the slopes of subglacial mountain ranges in the ice flow direction. There are local manifestations of the subglacial water layer (according to results of our airborne radio-echo sounding). The velocity of the ice sheet surface flow is from 10 to 40 m/year (Rignot et al., 2011, 2017). There is a steady direction of katabatic wind in the near-surface region in the direction of the ice sheet slope (almost along the direction of the ice flow line).

2.2. Basic research tools

A mobile research unit, provided with the necessary equipment and devices, was used in order to reach the regions and conduct research (Table 1).

2.3. Methods and research data

The access to the blue ice area is possible only by helicopter because the crevasse zone is spread 10 km long by 50 m wide.

On the other hand, ground vehicles are available to access to the blue firn area because cracks in this area there are in much smaller numbers than in the Blue Ice Area.

In both areas, the Blue Firn Area and the Blue Ice Area, the following activities were performed. Satellite images were analysed. Manned and unmanned aerial photography were conducted. Airborne radar profiling was performed. Visual analysis of the surface (from the aircraft, helicopter and from the surface) was conducted.

In the Blue Firn Area, the following areal studies were carried out. A ground-penetrating radar (GPR) survey was conducted. Surface tachometry (the horizontal and vertical positions measurement of points on the ice sheet surface relative to one another), hardness measurements, and thermometry (measurement of snow surface temperature) were performed. Initial monitoring of snow accumulation and ice dynamics (measurement of the surface of ice sheet moving velocity) was performed. Core and non-core drilling were performed. Density and temperature were measured using ice and/or snow core.

In the area of Blue ice studies were carried out at two points of the helicopter landing (Points No.1 and No.2 in Fig. 2, Fig. 3, Fig. 5), were performed measurement of ice surface temperature and drilling without coring.

The home station (base) for the mobile research unit was selected to

be at the point of intersection of latitude 69°45' with the longitudinal axis of the surface of BIAs in the Blue Firn Area. We named this the point "LiMPoPo base".

The main complex of surface research was carried out in the Blue Firn Area during the sled-tractor campaigns from December 24–26, 2017 and on January 16, 2018.

Two helicopter landings were also made in the Blue Ice Area on December 27, 2017 and January 02, 2018.

2.3.1. Satellite images

Based on the results of the analysis of satellite images a 3D model of the surface (plan size about 55 × 55 km) of the ice sheet in the Larsemann Hills area, the Blue Firn Area and Blue Ice Area (Fig. 3.1) was constructed. Both the Blue Firn Area and the Blue Ice Area stood out in the apparent blue colour and could be referred to as BIAs. The wave-like character of the surface, which is most likely associated with the surface structure of the subglacial mountain relief, was revealed.

2.3.2. Airborne radio-echo sounding

Based on the results of airborne radar profiling, a 2D radar section of the studied roughly 55 km long area was constructed at latitude 69°45' (Fig. 3.1, section A-A) taking into account the topography (altitude) of the ice sheet and bed rocks (Fig. 3.2).

Based on the analysis of the radar section, the following data results were revealed.

- 1) The surface height of the ice sheet: in the Blue Firn Area is about 750 m; in the Blue Ice Area about 400 m (Fig. 3.2).
- 2) The Blue Firn Area and Blue Ice Area regions are located (Fig. 3.2) on the slope of coastal dissipation of the ice sheet (the ice sheet thickness decreases from 600 m to 300 m). Above the expressed most intense slopes of the subglacial hills and mountain ranges of the bedrock, these slopes rise in the direction of the ice flow line. The elevation angle of the slopes of the bedrock relief is about 4–6° in the Blue Firn Area (near the dotted line “LiMPoPo base” in Fig. 3.2) and about 20–35° in the Blue Ice Area (near the dotted line “Point №2” in Fig. 3.2).
- 3) Along the ice flow line, the ice sheet (about 600 m in thickness) is transformed into an ice shelf (about 250–300 m in thickness). The thickness of the ice sheet decreases and the elevation difference of the mountain relief of the bedrock increases: in front of the Blue Firn Area by 550 m, in front of the Blue Ice Area by 400 m (Fig. 3.2). The firn layer thickness presumably about 250 m (contrast border by results of airborne radio-echo sounding (Fig. 3.2)). The layers of firn and ice (along the ice flow line) change the angle of inclination relative to the surface (Figs. 3.2, Fig. 3.3, Figs. 5.2 and 5.3). In front of the Blue Firn Area they are sub-parallel to the surface of the subglacial relief. Within and behind the Blue Firn Area and Blue Ice Area they have an angle of inclination to the surface (about 3.5–4°);
- 4) The region has a large number of ice cracks (symbol “1” in Fig. 3.2) that have a width of up to 50 m on the ice sheet surface. They are more common on the slope of the ice sheet above the mountain ridges of the bedrock.

2.3.3. Ground-penetrating radar (GPR) survey

Based on the results of GPR survey, a 500-m radar section was constructed for the explored Blue Firn Area at latitude 69°45' through the LiMPoPo base (Fig. 3.3) point.

GPR technique is the main geophysical method for studying the upper part of the glacier, especially for future construction of an ice and snow runway (Popov et al., 2017).

Based on the analysis of the radar section, the following data results were revealed along the ice flow line. In front of the Blue Firn Area, a layered structure parallel to the surface of the ice sheet can be observed. In this area, there is a distinct contrast boundary between snow and firn at a depth of about 0 ... 2 m (Figs. 3.3 and 5.3, the interval along a

Table 1
Equipment and devices used in the research.

Logistics		Equipment
Aircraft vehicles		aircraft: Basler BT-67 («601 XUE YING SNOW EAGLE») helicopter: SA 365 Dauphin
Ground vehicles		snowcat with passenger cabin: Pisten Bully 240 D snowcat with passenger cabin: Pisten Bully Polar 300 snowcat without passenger cabin: Pisten Bully Polar 300 sled with fuel tank (for 3 tons of fuel) sled with power station sled with galley and dining cabin sled with residential module for 8 beds sled with residential module for 6 beds
Studies		Devices
Airborne Radio-echo sounding		aircraft: Basler BT-67 («601 XUE YING SNOW EAGLE») radar profiling parameters: f waves = ~60 MHz; H flight = ~600 m; V aircraft = 250–300 km/h;
Aerial photography	Manned	aircraft: Basler BT-67 («601 XUE YING SNOW EAGLE») hardware characteristics: - video/photo camera, model: Elphel NC353L; - matrix: 5MPix; 1/2.5"; - resolution: 2592x1944@15fps; H flight = ~600 m
	Unmanned	unmanned aircraft Polar Hawk-IV unmanned quadcopter DJI Inspire 2 on the sled behind the snowcat Pisten Bully 240 D
Ground-penetrating radar (GPR) Survey		hardware characteristics: Ground-penetrating radar: GSSI (Geophysical Survey Systems Inc., USA) with systemic module SIR3000 with antenna 3101, operational frequency 900 MHz total station: Trimble M3 DR 5" penetrometer: AARI (Arctic and Antarctic Research Institute) electronic thermometer: Testo 105, accuracy $\pm 0.1^{\circ}\text{C}$ auger drill: Kovacs Mark II (Kovacs Enterprises, USA) electrically operated electronic scale, accuracy ± 0.01 g electronic thermometer: Testo 105, accuracy $\pm 0.1^{\circ}\text{C}$ drill: Kovacs Ice Thickness Kit (Kovacs Enterprises, USA), electrically operated
Surface tacheometry		
Surface hardness measurements		
Surface thermometry		
Core drilling		
Core density measurement		
Core thermometry		
Non-core drilling		
Initial monitoring stage for snow accumulation and ice dynamics		aluminium pipe-markers
Coordinates of the point in the plan		satellite receivers: GARMIN GPSmap 76Cx; eXplorist Pro 10; GARMIN GPSmap 60s with remote antenna GA 25MCX

horizontal scale 0–25 m). In the zone nearest to the Blue Firn Area, the crushing of ice layers into a synclinal fold can be observed. As a result of this crushing, parallel layers of firn acquire an inclination angle of 3° to the ice sheet surface (Figs. 3.3 and 5.3, the interval along a horizontal scale 25–120 m). Within the Blue Firn Area itself, firn layers come to the surface as a structure of parallel layers with an inclination angle to the surface of about 3° (Figs. 3.3 and 5.3, the interval along a horizontal scale 120–240 m). Behind the Blue Firn Area, the formation of a snow layer that gradually increases in thickness can be observed. The inclination angle of the snow-firn separating surface is about 0.6° , and a structure of parallel ice layers can be observed under the snow (firn) layers with an inclination angle of about 3° (Figs. 3.3 and 5.3, the interval along a horizontal scale 240–500 m).

2.3.4. Surface tacheometry (the horizontal and vertical positions measurement of points on the ice sheet surface relative to one another)

Based on the results of airborne radar and surface tacheometry analysis, it was determined that, with a general sub-horizontal orientation, the ice sheet surface in the Blue Firn Area and Blue Ice Area has its own specific features. 1) Along the ice flow line and the katabatic wind direction (East to West) at latitude $69^{\circ}45'$ (section A-A in Figs. 3.1 and 3.2) and the latitudinal direction lines, perpendicular to the longitudinal axis of the surface of BIAs (“BIAs axis”) (lines in Region A and B in Fig. 2.2, line 5 in Fig. 4.1 and dotted axis in Fig. 3.2), the surface incline angles change their “sign relative to the horizon” (“negative angle” - surface slope – down (the angle β and symbol “2” in Fig. 3.2),

“positive angle” - surface slope – up (the angle λ and symbol “3” in Fig. 3.2)). a) In Blue Firn Area (near the LiMPoPo base point in Fig. 3.1, at a point at a distance of 50 m in Fig. 3.3), In front of the Blue Firn Area (to the east of the “BIAs axis”) the surface slope is “negative” (descent, down) and angles reach $3\text{--}4^{\circ}$. Behind the Blue Firn Area (to the west of the “BIAs axis”) the surface slope is “positive” (elevation, up) and the angles reach $1\text{--}2^{\circ}$. b) In Blue Ice Area (near the Point №2 in Fig. 3.1): in front of the Blue Ice Area (to the east of the “BIAs axis”) the surface slope is “negative” (descent) and the angles reach $1\text{--}2^{\circ}$. Behind the Blue Ice Area (to the west of the “BIAs axis”) there is almost no surface slope – 0° . 2) Along the “BIAs axis” (lines in Region A and B in Fig. 2.2, line 5 in Fig. 4.1 and dotted axis in Fig. 3.2) the southern region is lower than the northern one and the surface inclination angle does not exceed a) 2° in Blue Firn Area or b) 1° in Blue Ice Area.

Thus, along the ice flow line and in the katabatic wind direction (East to West) at latitude $69^{\circ}45'$ and latitudinal direction lines, a “bend” (“concavity”) in the ice sheet surface can be observed, with a total concavity angle of a) $4\text{--}6^{\circ}$ in the Blue Firn Area (near the LiMPoPo base point in Fig. 3.2, at a point at a distance of 50 m in Fig. 3.3) and b) $1\text{--}2^{\circ}$ in Blue Ice Area (near the Point №2 in Fig. 3.2).

2.3.5. Surface hardness measurements

Based on the results of surface hardness measurements analysis to a depth of 1 m along the BIAs propagation axis in the Blue Firn Area (Fig. 4.1), the following results (Fig. 4.4) were revealed:

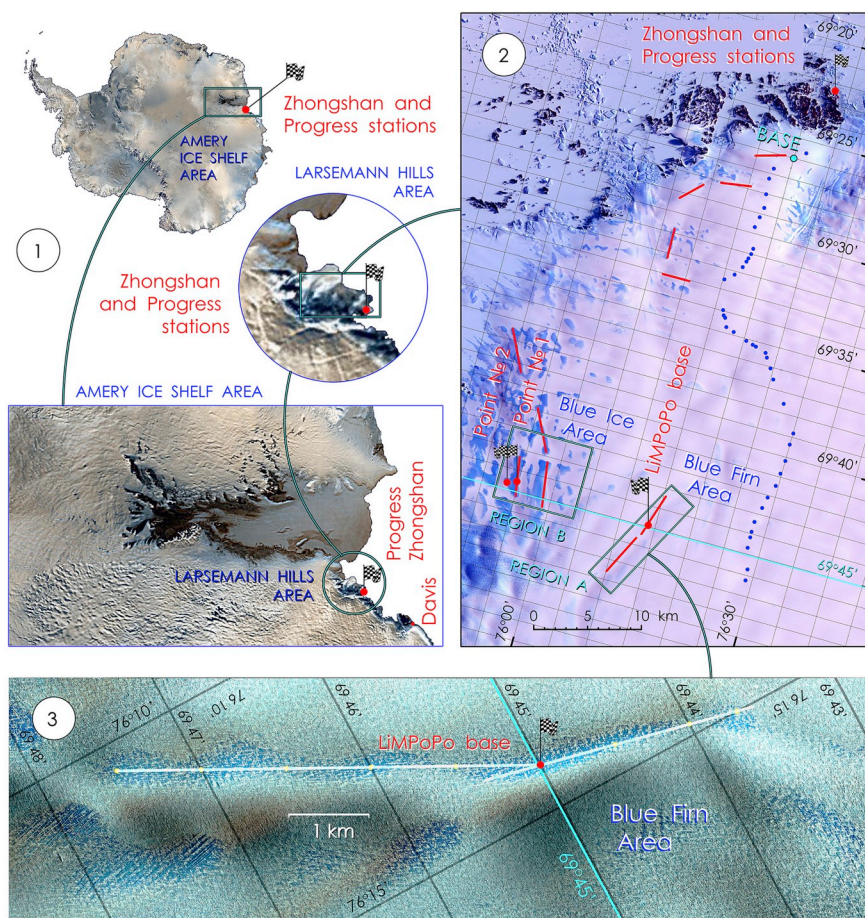


Fig. 2. Area of research: 1) Location of the Larsemann Hills area in Antarctica; 2) Location of the Blue Firn Area and the Blue Ice Area in the Larsemann Hill area (detailing about 15 m per pixel) (based on the satellite image courtesy of V.D. Klokov and from the archives of the Arctic and Antarctic Research Institute, Russia). The red lines indicate the preliminary places to search for BIAs. Region A and Region B have the most interesting BIAs of a linear length about 3 km. The blue dotted line indicates the route from the Progress (Russia) and Zhongshan (China) to Vostok (Russia) and Kunlun (China) Stations; 3) In the Blue Firn Area (Region A) (detailing about 0.5 m per pixel) (from the archive of Polar Research Institute of China (Shanghai, People's Republic of China)), the scale in Fig. 2.3 (relative to Fig. 2.2) increases in the proportion: 7/1. (For interpretation of the references to colour in this figure legend, the reader is referred to the Web version of this article.)

- 1) Throughout most of the region, surface hardness is higher than the snow cover hardness in surrounding areas, but lower than ice hardness, and corresponds to a firn hardness of 0.2 MPa
- 2) In the northern part of the region, the surface hardness is higher than that in the southern region and reaches 0.4 ... 0.6 MPa;
- 3) In the northern part of the region, firmer firn layers rise closer to the surface; in the section depth along the axial line, an increase in hardness up to 0.6 MPa occurs in the southern part of the region at a depth of about 60 ... 80 cm, and in the northern part this increase is observed at a depth of about 30 cm and reaches a depth of 60 ... 80 cm with values of 0.8 ... 1.0 MPa.

General analysis of the hardness of the section to a depth of 1 m showed that no open outcrop of the Blue Ice can be observed in the region.

The surface hardness in the upper part of the section (a depth of less than 1 m) corresponds to the firn hardness.

However, a significant part of the surface is covered with a sun crust, and, accordingly, has a pronounced blue colour and icy shine. In connection with this, the entire region was conventionally named as the Blue Firn Area.

2.3.6. Surface snow and ice temperature

Based on the temperature measurement of the depth of 4 cm and 19 cm in nine points at the BIAs propagation axis in the Blue Firn Area (Fig. 4.1), the following results were revealed (Fig. 4.5):

- 1) The average temperature along the entire axis is -4.75°C ;
- 2) The surface temperature in the southern and central parts of the axis (the average is around -5.38°C) is approximately 2° lower than that in the northern part (the average is around -3.48°C);

- 3) The average temperature increase gradient along the entire axis with a depth decrease (from 19 to 4 cm) is $3.07^{\circ}/\text{m}$ (the temperature increases when approaching the surface);
- 4) The average temperature increase gradient with decreased depth in various areas of the axis has a different value and even "changes the sign":
 - In the southern region, the average gradient is negative $-2.44^{\circ}/\text{m}$ (the temperature decreases when approaching the surface);
 - In the central region, the average gradient is positive $4.44^{\circ}/\text{m}$ (temperature increases when approaching the surface);
 - In the northern region, the average gradient is positive $7.22^{\circ}/\text{m}$ (temperature increases when approaching the surface).

2.3.7. Core drilling

Based on the results of analysis for the cores of three boreholes drilled to a depth of 6 m (at the LiMPoPo base point and 1 km north (No. 03-03-b) and south (No. 03-05-b) from the LiMPoPo base point along the BIAs propagation axis in the Blue Firn Area (Fig. 4.1), the temperature and density of the snow-firn ice layer was recorded up to a depth of 6 m.

2.3.8. Core density measurement

Based on the results of snow density determination of core, the following (Fig. 4.2) was detected:

- Core density in all three boreholes increases with depth (on the average) from about $500\text{ kg}/\text{m}^3$ (near the surface) to about $650\text{ kg}/\text{m}^3$ (at a depth of 5 m);
- Core density in the southern borehole (No. 03-05-b) over the entire depth is less than in the central (No. 03-04-b) and northern (No. 03-03-b) boreholes, approximately by $50\text{ kg}/\text{m}^3$;

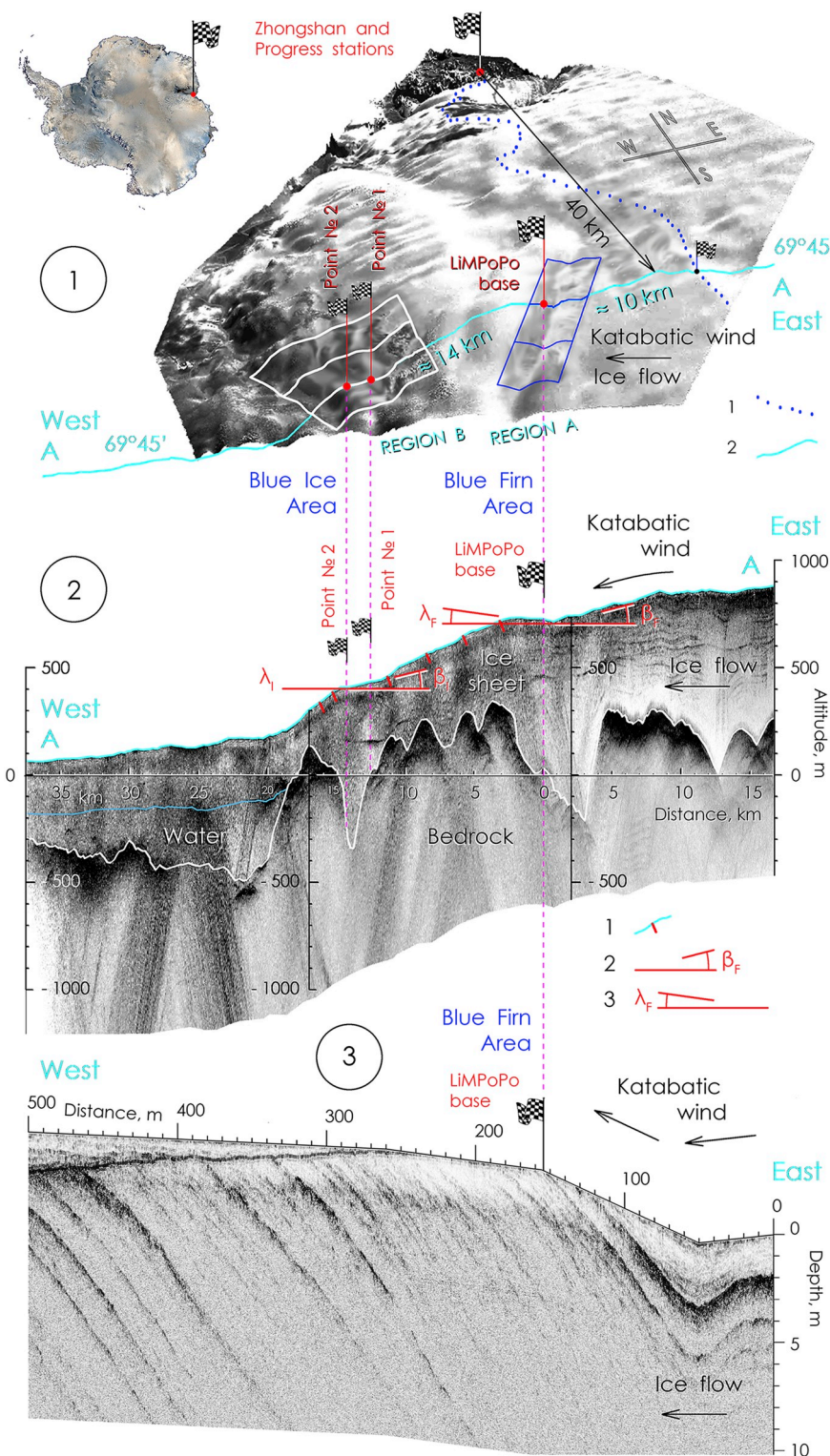


Fig. 3. Research results: 1) 3D model (based on the satellite images) of the surface of the Larsemann Hills area: 1 indicates the route from the Progress Station (Russia) and Zhongshan (China) to Vostok Station (Russia) and Kunlun (China) Stations; 2 indicates the line of latitude 69°45' of the Blue Firn Area and Blue Ice Area (in the Larsemann Hills area) through the LiMPoPo base point. 1 - indicates the region of ice cracks (red inclined line on the surface of the ice sheet); 2 - β_F and β_I indicate “negative surface incline angles” - surface slope - down.; 3 - λ_F indicates “positive surface incline angle” - surface slope - up, or λ_I indicates “0” surface incline slope - horizontally; 3) 2D ground-penetrating radar (GPR) section at latitude 69°45' in the Blue Firn Area through the LiMPoPo base point. The light grey layer which is parallel to the surface (to a depth of 2 m) is due to the GPR device. The scale in Fig. 3.3 (relative to Fig. 3.2) increases in the proportion: 100/1. . (For interpretation of the references to colour in this figure legend, the reader is referred to the Web version of this article.)

- Core density in all three boreholes at a depth of about 2–3 m reaches 600 kg/m³;
- In the southern well (No. 03-05-b), starting from 4 m and lower, there are layers with a density of about 800 kg/m³, which are ice.

Thus, up to a depth of about 6 m, core density practically corresponds to the firn density. However, in the southern borehole (No. 03-05-b), starting from 4 m and below, there are layers (up to 20 cm thickness) of ice and their density corresponds to ice (Table 2).

2.3.9. Core thermometry (temperature measurement inside the core of the boreholes)

Snow temperature measurements were made at the time of core extraction from a borehole, measuring point was inside the core at a distance of 3 cm from its side surface.

Based on the results of measurement temperature inside the core, the following (Fig. 4.3) was detected:

- Snow temperature decreased with depth in all three boreholes (on

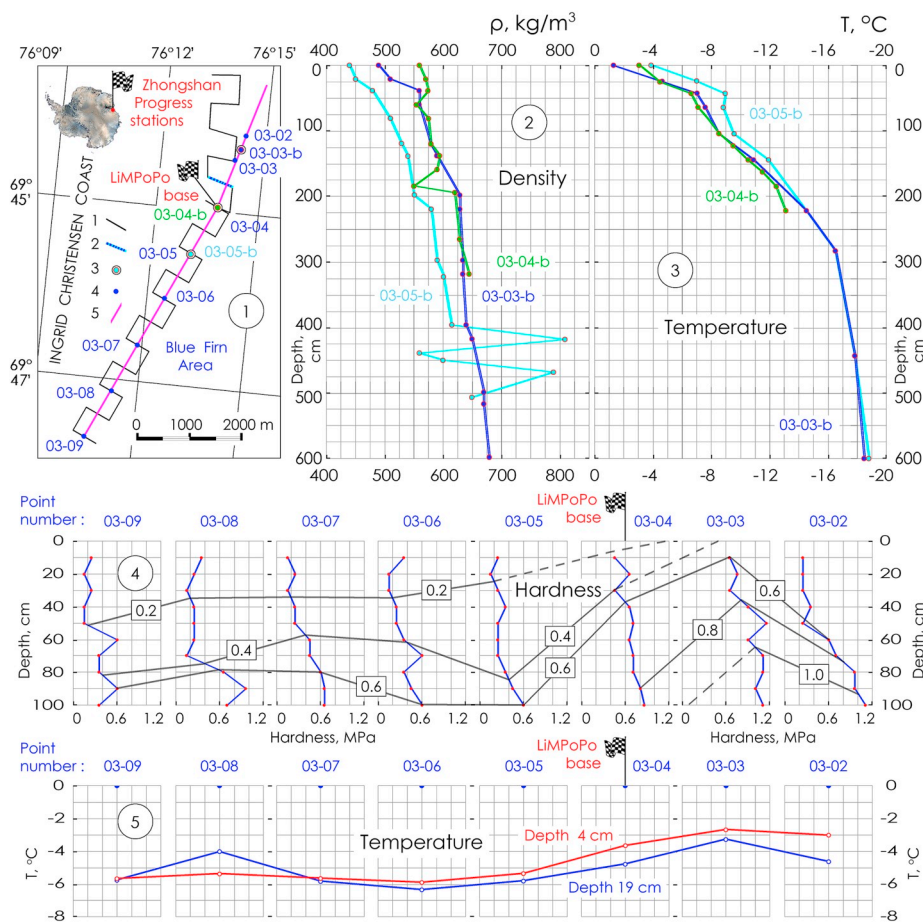


Fig. 4. Research results: 1) The Blue Firm Area orientation scheme and location where research was conducted: 1 – Profiles (traces) of georadar profiling at the surface; 2 – Profile (trace) through the LiMPoPo base point for which the radar section was constructed, as shown in Fig. 3.3; 3 – Points of core drilling to a maximum depth of 6 m; 4 – Surface hardness measurement points; 5 – BIAs propagation axis in the Blue Firm Area; 2) Snow density profiles at the points 03-03-b, 03-04-b and 03-05-b in Fig. 4.1; 3) Snow temperature profiles at the points 03-03-b, 03-04-b, and 03-05-b in Fig. 4.1; 4) Snow hardness profiles at the points (pickets 03-09 ... 03-02 in Fig. 4.1) on the surface at the BIAs propagation axis (line 5 in Fig. 4.1) in the Blue Firm Area (layers of different hardness are marked); 5) Snow temperature profiles at the points (pickets 03-09 ... 03-02 in Fig. 4.1) on the surface at the BIAs propagation axis (line 5 in Fig. 4.1) in the Blue Firm Area (Fig. 4.1).

average) from about -3°C (near the surface) to about -18°C (at a depth of 5 m);

- Snow temperature in the southern borehole (No. 03-05-b) (to a depth of about 2 m) is lower than in the central (No. 03-04-b) and northern (No. 03-03-b) boreholes by approximately 1.5°C , and below a depth of 2 m the temperature in the southern (No. 03-05-b) and northern (No. 03-03-b) boreholes is almost the same;
- The temperature gradient over the depth of all boreholes does not change equally: the most intense temperature change is observed at depths from 0 to 2.75 m where the temperature gradient is about $4.7^{\circ}/\text{m}$; below 2.75 m the temperature increase is less intensive, and the temperature gradient is about $0.6^{\circ}/\text{m}$. It should be noted that the upper, more gradient layer of temperature change (at depths from 0 to 2.75 m) corresponds to a core consisting of “large rounded particles (RGlR) with ice inclusions in the form of an ice column (IFic),” and the core below the depth of 2.75 m corresponds to a core consisting of “large rounded particles (RGlR);”
- Based on curvature and extrapolation below a depth of 6 m on temperature graphs for all three boreholes, it can be assumed that inversion occurs at a depth of about 7–8 m (change of the gradient sign) and temperature increases with depth, i.e. the “seasonal” layer of temperature fluctuations has a thickness of about 7–8 m.

2.3.10. Structural analysis of the core (Table 2)

Core texture analysis revealed that the following results:

- Firm with individual ice inclusions in the form of ice layers and lenses can be observed along almost the entire depth of all three boreholes;
- Firm porosity decreases with depth;
- Above a depth of about 2 m, alternating layers were found in all

three boreholes with “large rounded particles (RGlR) with ice inclusions in the form of an ice column (IFic)” (a higher temperature gradient of about $4.7^{\circ}/\text{m}$ is also observed in this interval);

- In the central borehole (No. 03-04-b) at a depth of 1.85 m, there is a layer (10 cm thickness) of “deep hoarfrost in the form of hollow cup-shaped crystals (DHcp)” (with a local decrease in density up to about $550\text{ kg}/\text{m}^3$);
- The “large rounded particles (RGlR)” core structure is observed below a depth of about 2 m in all three boreholes (the temperature gradient in this interval decreases to about $0.6^{\circ}/\text{m}$ compared to the overlying strata);
- In the southern borehole (No. 03-05-b), at a depth interval of 4 m–5 m, two layers are observed (20 cm and 40 cm thickness) of “ice inclusion in the form of an ice column (IFic)” (density of about $800\text{ kg}/\text{m}^3$), and at a depth of 4.4 m, a layer of deep hoarfrost about 10 cm thickness can be observed. Those are followed by layers of firm in the form of “hollow cup-shaped crystals (DHcp)” (with a local decrease in density up to $550\text{ kg}/\text{m}^3$).

2.3.11. Initial monitoring stage for snow accumulation and ice dynamics

In order to conduct annual monitoring of snow accumulation and ice sheet surface dynamics, aluminium pipe-markers were installed at nine points located in the Blue Firm Area (Fig. 4.4).

2.3.12. Visual analysis

After traveling by helicopter to two different points of the Blue Ice Area (about 2 km from each other) (points in Region B in Fig. 2.2) located on the BIAs axial line, drilling to a depth of 1 m, surface temperature measurement and a detailed visual analysis of the ice sheet surface were carried out.

In the Blue Ice Area, an outcrop of glacier ice without snow with an

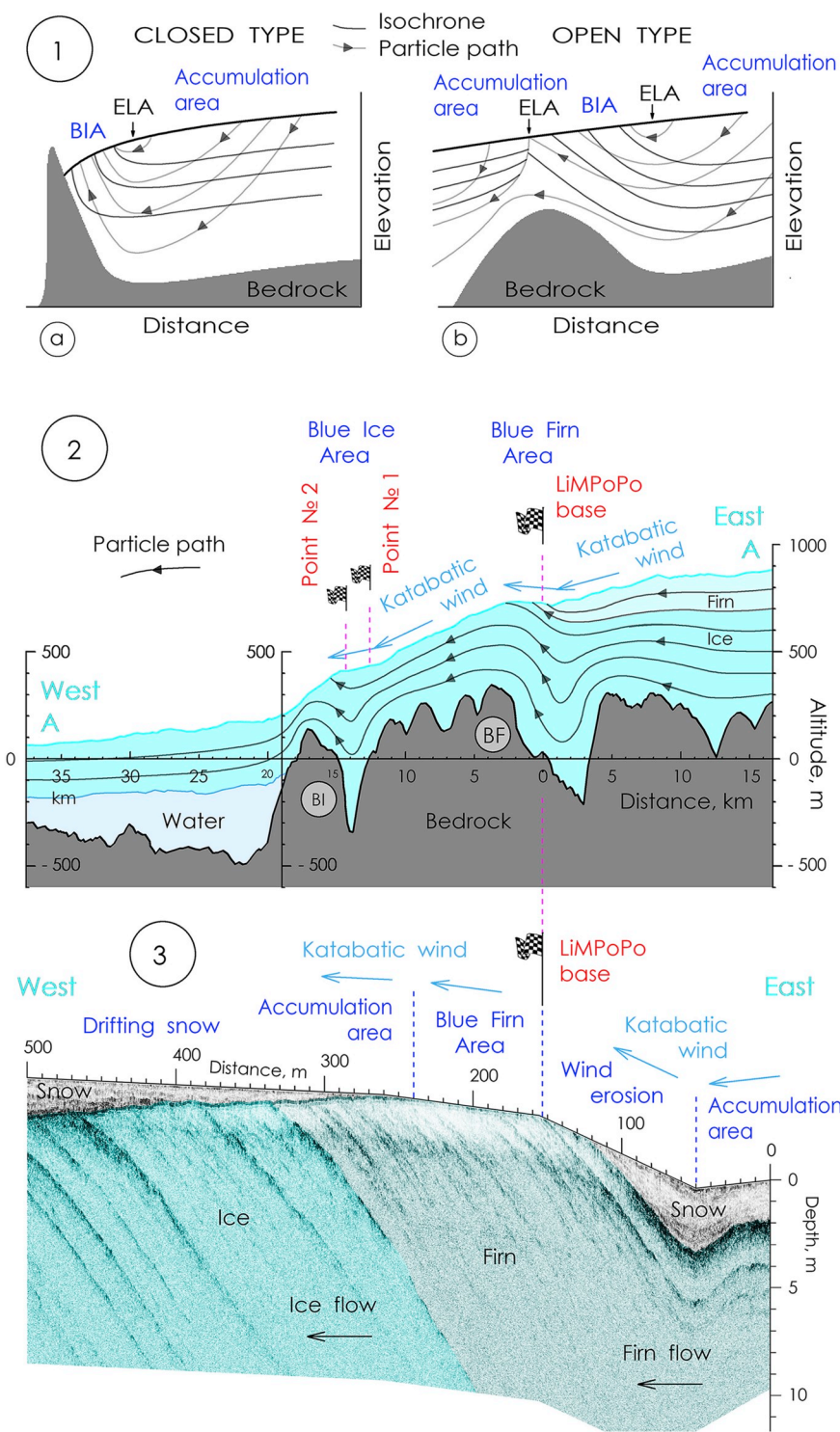


Fig. 5. Conditions for the formation and preservation of BIAs: 1) The main two categories of conditions for the existence of BIAs (Bintanja, 1999; Sinisalo and Moore, 2010) (ELA - equilibrium line); 2) A schematic section (about 55 km long) of conditions for the formation and preservation of BIAs at latitude 69°45' for the Blue Firn Area and Blue Ice Areas (subglacial mountain ranges (the root cause of the formation of BIAs): BF - in the Blue Firn Area; BI - in the Blue Ice Area); 3) A schematic section (about 500 m long) of conditions for the formation and preservation of BIAs at latitude 69°45' for the Blue Firn Area through the LiMPoPo base point. The boundary between firn and ice layers is highlighted on the contrast boundary of the radar reflection. The scale in Fig. 5.3 (relative to Fig. 5.2) increases in the proportion: 100/1.

almost smooth surface (with insignificant waviness) was observed. The dimensions of each of the two BIAs (in which the researchers landed) are about 2 × 5 km (as reflected in Fig. 2.2).

The surface of the BIAs is almost horizontal. There are a large number of cracks on the BIAs periphery.

The surface temperature at the landing points in the Blue Ice Area was about - 1 °C–2 °C.

3. Analysis of research data

We carried out a comprehensive comparison of the observed

conditions and parameters in the Blue Firn Area and in the Blue Ice Area (Table 3) to determine differences or similarities in the causes of the formation of BIAs.

The explored Blue Firn Area and Blue Ice Area have the same type of features:

- 1) They are located at almost the same latitude (69°45'). They are on almost one line of the ice sheet flow. They are in the territory that adjoins the Amery Ice Shelf area in the Larsemann Hills area. The axial lines of the Blue Firn Area (lines in Region A in Fig. 2.2) and the axial lines of the Blue Ice Area (lines in Region B in

Table 2
Analysis data for the core taken from boreholes: No. 03-05-b; No. 03-04-b; No. 03-03-b.

Core from well No. 03-05-b				Core from well No. 03-04-b				Core from well No. 03-03-b			
H (cm)	FF	E (mm)	ρ kg/m ³	H (cm)	FF	E (mm)	ρ kg/m ³	H (cm)	FF	E (mm)	ρ kg/m ³
0	RGlR	2.0–3.0	440	0	RGlR-IFic	1.5–2.5	560	0	RGlR	1.5–2.5	490
–20	RGlR-IFic	1.5–2.5	450	–20	RGlR-IFic	1.0–2.0	570	–20	RGlR-IFic	1.5–2.5	510
–40	RGlR	1.5–2.5	480	–40	RGlR-IFic	1.0–2.0	575	–40	RGlR-IFic	1.5–2.5	560
–80	RGlR	1.0–2.0	510	–60	RGlR-IFic	1.0–2.0	555	–60	RGlR	1.0–2.0	560
–120	RGlR-IFic	1.0–2.0	530	–80	RGlR	1.0–2.0	575	–120	RGlR-IFic	1.0–2.0	580
–140	RGlR	1.0–1.5	540	–120	RGlR	1.0–2.0	580	–140	RGlR	1.0–2.0	590
–200	RGlR-IFic	1.0–2.0	550	–140	RGlR-IFic	1.5–2.5	595	–200	RGlR-IFic	1.0–2.0	630
–220	RGlR	0.5–1.5	580	–160	RGlR	1.5–2.5	590	–220	RGlR	0.5–1.5	630
–300	RGlR	1.0–2.0	590	–185	DHcp	2.0–3.0	550	–300	RGlR	1.0–2.0	635
–320	RGlR	0.5–1.0	600	–195	RGlR	1.0–2.0	620	–320	RGlR	1.0–2.0	635
–400	RGlR	1.0–2.0	615	–270	RGlR	1.0–2.0	630	–400	RGlR	1.0–2.0	640
–420	IFil	1.0–2.0	810	–320	RGlR	1.0–2.0	645	–420	RGlR	1.0–2.0	650
–440	DHcp	3.0–5.0	560	–345				–500	RGlR	1.0–2.0	670
–450	RGlR	1.0–2.0	600					–520	RGlR	1.0–2.0	670
–470	IFil	1.0–2.0	790					–600	RGlR	1.0–2.0	680
–510	RGlR	1.0–2.0	650					–670			
–600											

H - depth of snow cover.
L - layer thickness.
FF - morphological classification (grain characteristics).
E – grain size.
 ρ - density.
RGlR - large rounded particles.
DHcp - deep hoarfrost in the form of hollow cup-shaped crystals.
IFic - ice inclusion in the form of an ice column.

Table 3
Comparing characteristics between the blue firn area and blue ice area.

Characteristics	Blue Firn Area	Blue Ice Area
Surface altitude above sea level	750 m	400 ... 450 m
Geographic latitude	69°45'	
Ice sheet surface temperature in the daytime	about – 4.75 °C	about -2-3 °C
Surface colour	Slightly blue	Very blue
Morphological characteristics of the areas	located on the slope of the coastal “dissipation” of the ice sheet (sheet thickness decreases from 600 m to 300 m) along the ice flow line over the ice sheet area thickness about 600 m) and transforms into an ice shelf (thickness about 250 ... 300 m) over the most intensely sized mountain ranges, which rise in the direction of the ice flow line	
The shape of subglacial mountain relief		
The elevation angle of the slopes of bed relief mountain ranges	up to 4–6°	up to 20–35°
Decrease in the ice sheet thickness in the ice flow direction before and above the subglacial mountain range	by 550 m (from 950 m to 400 m)	by 400 m (from 750 m to 350 m)
Elevation difference of the subglacial mountain relief based on the ice flow line up to the ridge	by 550 m (from – 200 m to + 350 m)	by 400 m (from 350 m to 50 m)
Longitudinal axis direction	± 25° from the direction of the meridian	
Longitudinal axis length	about 3 ... 5 km	
Ice flow direction	East to West (perpendicular to the axis of subglacial mountain range)	
Surface velocity	3 ... 4 m/year	80 ... 100 m/year
Wind direction (dominant)	Eastern (perpendicular to the axis of glacier surface bend)	
“Bend” (“concavity”) of the ice sheet surface along the ice flow line and in the katabatic wind direction at latitude 69°45' and the latitudinal direction lines, total angle of the surface “bend” (“concavity”)	about 4–6°	about 2°

Fig. 2.2) have a nearly parallel submeridional direction, and approximately the same length of about 3 ... 5 km;
2) Daytime temperatures on the ice sheet surface in both areas is negative and not below 5 °C;
3) The ice sheet surfaces are almost horizontal;
4) The ice sheet is partially fractured;
5) The colour of the ice sheet surface along the axial lines of both areas in satellite images is blue, characteristic for BIAs.

The explored Blue Firn Area and Blue Ice Area have some differences:

- 1) The Blue Firn Area has an altitude of about 750 m, and the Blue Ice Area has an altitude of about 400 ... 450 m;
- 2) The BIAs area in the Blue Ice Area is significantly larger than in the

- Blue Firn Area;
- 3) The surface of the Blue Ice Area more orthogonal (approximate by 2°) to the flow of the solar radiation than does the surface of the Blue Firn Area;
- 4) The daytime temperature on the ice sheet surface in the Blue Ice Area is 2–3 °C higher than in the Blue Firn Area;
- 5) The flow velocity of the ice sheet surface in the Blue Firn Area is about 3 ... 4 m/year, and in the Blue Ice Area - about 80 ... 100 m/year (Rignot et al., 2011, 2017);
- 6) The surface of the Blue Ice Area has more ice cracks than the surface of the Blue Firn Area;
- 7) The Blue Firn Area has a more pronounced blue colour in the satellite images than does the Blue Ice Area.

Analysis of the likely dominance of any of the various formation

factors of BIAs known from research results in other areas was performed (Bintanja, 1999; Bintanja and Reijmer, 2001; Hui et al., 2014; Sinisalo and Moore, 2010; Takahashi et al., 1988; Winther et al., 2001; Winter et al., 2016; Zwinger et al., 2014).

4. Results

Since more intensive dynamics is one of the specific conditions for the existence of the ice sheet in the coastal zone as compared with internal areas, the conditions for the formation and existence of BIAs should be considered by the analysis of the specific features of the ice sheet flow in local BIAs.

Comprehensive analysis of the data obtained makes it possible to identify the genesis of BIAs in the Blue Firn Area and Blue Ice Area.

Both areas belong to the “Open Type” (Bintanja, 1999; Sinisalo and Moore, 2010) (Fig. 5.1) BIAs category. The main unique conditions for this BIAs category are the ice sheet flowing through the subglacial mountain range (mountain peak), which is located within the ice (does not come to the surface) (Fig. 5.2).

With this research, we found that, in the direction of the ice flow line and of the katabatic wind (East to West) (at latitude 69°45'), the following transformations of the internal and external conditions of the ice sheet (Figs. 5.2 and 5.3) flow take place in the Blue Firn Area and Blue Ice Area that we studied:

- 1) For the entire flow line there is a decrease in the total thickness of the ice sheet, in connection with which the influence of the surface structure of the subglacial mountain relief on the ice flow structure increases throughout the entire thickness of the ice sheet (and not only in the lower, bottom layer) (Fig. 5.2). There is also sequential flow over two subglacial mountain ranges (in the Blue Firn Area (BF) (Fig. 5.2) and Blue Ice Area (BI) (Fig. 5.2)), located perpendicularly (like barriers) to the flow line.
- 2) Within the Blue Firn Area the sub-horizontal position of the firn and ice layer surfaces becomes angled to the ice sheet surface due to the flow through the subglacial mountain range (BF) (Fig. 5.2). Right above the subglacial mountain range, the ice sheet surface also changes the angle of inclination (“rises”), as a result of which a deflection (“barrier,” “step”) is formed perpendicular to the line of the dominant flow of the katabatic wind (Fig. 5.1b and Fig. 5.2).

On a relatively steep ice sheet surface (“barrier,” “step”) caused by bedrock under the ice sheet, a stronger katabatic wind blows on the surface and causes larger snow drift transport rate (“drifting snow”), by which snow surface is eroded (area of “Wind erosion” in Fig. 5.3) to make a bare firn and ice surface. However, “wind” cannot erode ice. The formed bare ice surface is subject to sublimation due to its low albedo. Drifting snow and wind erosion causes the firn (and partial ice) layers to be exposed at the surface (“BIA” in Fig. 5.1b and “Blue Firn Area” in Fig. 5.3).

Meteorological conditions on the surface (temperature, insolation, wind velocity) within the Blue Firn Area create conditions that prevent significant accumulation of snow on the surface of the exposed firn (partially ice) (mass balance area close to zero). Nevertheless, the complex impact of the formation and maintenance factors of BIAs is insufficient for the sustainable existence of BIAs, thus only firn is observed on the surface.

- 3) Behind the Blue Firn Area a “reverse bend” (“lowering”) of the slope surface occurs, and a wind shadow area forms. A significant accumulation of “drifting snow” occurs in this area (area of positive mass balance of “drifting snow” in Fig. 5.3). The snow covers the ice in the absence of a firn layer above the ice, which was blown away due to wind erosion (Fig. 5.1b and Fig. 5.3).
- 4) Within the Blue Ice Area the firn and ice layers become even more inclined to the ice sheet surface due to repeated flowing through the

subglacial mountain range (BI) (Fig. 5.2). Right above the subglacial mountain range, the ice sheet surface again changes the inclination angle (“rises”) (similarly to the Blue Firn Area), resulting in the formation of a similar deflection (“barrier,” “step”) along the line of the dominant flow of the katabatic wind (Fig. 5.1b and Fig. 5.2). Under the wind load (of the katabatic wind) on a relatively steep ice sheet surface (“barrier,” “step”) the layer of “drifting snow” (that accumulated behind the Blue Firn Area) is destroyed (area of negative mass balance, “wind erosion”) (Fig. 5.1b and Fig. 5.2). As a result of this wind erosion, ice layers are “exposed” at the surface now without firn, which was previously destroyed (subjected to wind erosion) in the Blue Firn Area (Fig. 5.1b and Fig. 5.2). Meteorological conditions on the surface (temperature, insolation, wind velocity) within the Blue Ice Area create conditions preventing snow accumulation on the “exposed” ice surface (area of negative mass balance). The complex impact of the formation and sustaining factors of BIAs is sufficient for the sustainable “comfortable” existence of BIAs, and therefore only ice is observed on the surface.

The ice sheet that alternately flows “in waves” (Fig. 5.2) over the subglacial mountain ranges in the Blue Firn Area and Blue Ice Area is “subjected” to “cleaning” (in several stages) from snow and firn (“wind erosion” and “drifting snow”). The degree of “wind erosion” is not enough to form BIAs in the Blue Firn Area. However the “cleaning” in the Blue Ice Area takes place anew, in conditions that are more suited to preserve BIAs on the surfaces (strong katabatic wind sweeps drifting snow from a bare ice surface). Therefore, already in the Blue Ice Area the degree of “wind erosion” is enough to form BIAs.

Though “clean” ice does not emerge on the surface in the Blue Firn Area, its location (judging by data from the radar section (Figs. 3.3 and 5.3)) is close to the surface and is blocked only by a relatively thin layer (up to 2 m) of “drifting snow”.

It is likely that, with minor changes in conditions (reduction of snow accumulation or increase in wind erosion) in the Blue Firn Area, ice will be “exposed” on the surface.

In regard to the above, we can state the following:

- 1) The following conditions are required for the formation and maintenance of BIAs: exposure of the ice surface, i.e. destruction, “wind erosion” of the upper layers of snow and firn (negative mass balance on the surface); and “preservation” of the ice surface, i.e. no snow accumulation on the “exposed” ice surface (“drifting snow”, sublimation, zero or negative mass balance on the surface).
- 2) The main factors that cause “exposure” of the ice surface and formation of BIAs are as follows (in sequence of significance). There are structural factors (“elevation” of ice layers in the flow to the surface above the “steps” of the relief of subglacial mountain ranges); and there are meteorological factors (wind erosion, “drifting snow”).
- 3) The main factors that cause the preservation of BIAs with no snow accumulation are as follows (in sequence of significance). The meteorological factors are wind erosion, “drifting snow”, temperature, insolation, and sublimation. The structural factors are the favourable inclination angles of the ice sheet surface to create wind load on the surface.

5. Discussion and conclusion

In the area under study, the primary causes (necessary conditions) for the formation of BIAs are the structural changes in the ice flow over local subglacial mountain ranges and the wind erosion of the ice sheet surface as it flows through these subglacial mountain ranges, if there are additional (sufficient) conditions for meteorological parameters and slope of the ice sheet surface.

The surface in the Blue Firn Area, which we initially marked as BIAs according to the results of the analysis of satellite images and even the results of visual analysis of the surface from the aircraft, turned out not

to be a surface of ice, but firn (with a sun crust on the surface).

The analysis of satellite images and aircraft observation is not enough for reliable zoning of the BIAs distribution areas. Glaciological and radar surveys on the surface are necessary.

The formation and existence of BIAs in the study area can be fully explained by the local conditions of the coastal zone of the ice sheet, which can occur on the periphery of the ice sheet during different climatic “eras” (cooling or warming), i.e. be a “quasi-permanent” form of BIAs on the ice sheet surface.

Where there is “quasi-permanence” of the “necessary” structural conditions for the formation of BIAs (“elevation” of ice layers in the flow to the surface above the “steps” of the relief of subglacial rocks), the expansion or reduction of BIAs may occur due to changes in the sufficient local meteorological conditions of BIAs “preservation” (wind erosion) on the surface in a local area.

The conclusions for making an ice runway for heavy aircraft from the results of this study are as follows. 1) The Blue Firn Area (Region A in Fig. 2.2) is not a “BIAs” surface. The hardness of the surface is not enough for making ice runway for heavy aircraft (the critical condition for setting runway: the hardness - not less 1.0 MPa); It is necessary to conduct work to increase surface hardness. 2) The Blue Ice Area (Region B in Fig. 2.2) is a “BIAs” surface. However, the area has a large number of ice cracks (up to 25% of the surface area). It is necessary to conduct detailed geodesic, engineering, glaciological and geophysical studies to choose a place for an ice runway.

Acknowledgements

This study was partly funded by RFBR according to the research project No 16-05-00579_a.

We are very grateful to the following individuals for their assistance in conducting research in Antarctica:

- research engineers: Li Yuansheng (People's Republic of China);
- crew of aircraft BT-67 601 XUE YING SNOW EAGLE: commander William Houghton (Canada); co-pilot Zachary Young (Canada); flight engineer Chris John (Canada).
- crew of helicopter SA 365 Dauphin (People's Republic of China).
- driver mechanics of the Chinese Antarctic Expedition (People's Republic of China).

References

Bintanja, R., 1999. On the glaciological, meteorological and climatological significance of

- Antarctic blue ice areas. *Rev. Geophys.* 37 (3), 337–359.
- Bintanja, R., Reijmer, C.H., 2001. Meteorological conditions over Antarctic blue-ice areas and their influence on the local surface mass balance. *J. Glaciol.* 47 (156), 37–50. <https://doi.org/10.3189/172756501781832557>.
- Cassidy, W., Harvey, R.P., Schutt, J., Delisle, G., Yanai, K., 1992. The meteorite collection sites of Antarctica. *Meteoritics* 27 (5), 490–525.
- Fireman, E.L., 1989. The Lewis Cliff meteorite stranding area, polar ice cores and Wisconsin period impacts. *Lunar Planet. Sci.* 21, 365–366.
- Hui, F.M., Ci, T.Y., Cheng, X., Scambos, T.A., Liu, Y., Zhang, Y.M., Chi, Z.H., Huang, H.B., Wang, X.W., Wang, F., Zhao, C.C., Jin, Z.Y., Wang, K., 2014. Mapping blue ice areas in Antarctica using ETM+ and MODIS data. *Ann. Glaciol.* 55 (66), 129–137. <https://doi.org/10.3189/2014AoG66A069>.
- Mellor, M., Swithinbank, C., 1989. Airfields on Antarctic glacier ice. *CRREL Rep.* 89-21.
- Moore, J.C., Nishio, F., Fujita, S., Narita, H., Pasteur, E., Grinstead, A., Sinisalo, A., Maeno, N., 2006. Interpreting ancient ice in a shallow ice core from the South Yamato (Antarctica) blue ice area using flow modeling and compositional matching to deep ice cores. *J. Geophys. Res.* 111 (16). <https://doi.org/10.1029/2005JD006343>. PD16302/1-D16302/17.
- Nishiizumi, K., Jull, A.J.T., Bonani, G., Suter, M., Wölfli, W., Elmore, D., Kubik, P.W., Arnold, J.R., 1989. Age of Allan Hills 82102, a meteorite found inside the ice. *Nature* 340 (6234), 550–552. <https://www.nature.com/articles/340550a0.pdf>.
- Popov, S.V., Polyakov, S.P., Pryakhin, S.S., Mart'yanov, V.L., Lukin, V.V., 2017. The structure of the upper part of the glacier in the area of a snow-runway of Mirny Station, East Antarctica (based on the data collected in 2014/15 field season). *Earth's Cryosphere XXI* (1), 67–77. [https://doi.org/10.21782/EC2541-9994-2017-1\(67-77.2017](https://doi.org/10.21782/EC2541-9994-2017-1(67-77.2017)
- Rignot, E., Mouginot, J., Scheuchl, B., 2011. Ice flow of the Antarctic ice sheet. *Science* 333 (6048), 1427–1430. <https://doi.org/10.1126/science.1208336>.
- Rignot, E., Mouginot, J., Scheuchl, B., 2017. MEaSUREs InSAR-based Antarctica ice velocity map, version 2, Boulder, Colorado USA, NASA National snow and ice data center distributed active archive center. <https://doi.org/10.5067/D7GK8F5J8M8R>.
- Sinisalo, A., Moore, J.C., 2010. Antarctic blue ice areas - towards extracting palaeoclimate information. *Antarct. Sci* 22 (2), 99–115. <https://doi.org/10.1017/S0954102009990691>.
- Takahashi, S., Naruse, R., Nakawo, M., Mae, S., 1988. A bare ice field in east Queen Maud Land, Antarctica, caused by horizontal divergence of drifting snow. *Ann. Glaciol.* 11, 156–160. <https://doi.org/10.3189/S0260305500006479>.
- Van Roijen, J.J., van der Borg, K., de Jong, A.F.M., Oerlemans, J., 1995. Ages and ablation and accumulation rates from ¹⁴C measurements on Antarctic ice. *Ann. Glaciol.* 21, 139–143.
- Whillans, I., Cassidy, W., 1983. Catch a falling star: meteorites and old ice. *Science* 222, 55–57. <https://doi.org/10.1126/science.222.4619.55>.
- Winther, J.-G., Jespersen, M., Liston, G., 2001. Blue-ice areas in Antarctica derived from NOAA AVHRR satellite data. *J. Glaciol.* 47 (157), 325–334. <https://doi.org/10.3189/172756501781832386>.
- Winter, K., Woodward, J., Dunning, S.A., Turney, C.S.M., Fogwill, C.J., Hein, A.S., Gолledge, N.R., Bingham, R.G., Marrero, S.M., Sugden, D.E., Ross, N., 2016. Assessing the continuity of the blue ice climate record at Patriot hills, Horseshoe valley, west Antarctica: GPR assessment of Patriot hills BIA. *Geophys. Res. Lett.* 43, 2019–2026. <https://doi.org/10.1002/2015GL066476>.
- Zwinger, T., Schäfer, M., Martín, C., Moore, J.C., 2014. Influence of anisotropy on velocity and age distribution at Scharffenbergbotnen blue ice area. *The Cryosphere* 8, 607–621. <https://doi.org/10.5194/tc-8-607-2014>.